

# Seismic response of dual structures comprised by Buckling-Restrained Braces (BRB) and RC walls

Hamid Beiraghi\*

Department of Civil Engineering, Mahdishahr Branch, Islamic Azad University, Mahdishahr, Iran

(Received April 19, 2019, Revised June 20, 2019, Accepted June 22, 2019)

**Abstract.** In order to reduce the residual drift of a structure in structural engineering field, a combined structural system (dual) consisting of steel buckling-restrained braced frame (BRBF) along with shear wall is proposed. In this paper, BRBFs are used with special reinforced concrete shear walls as combined systems. Some prototype models of the proposed combined systems as well as steel BRBF-only systems (without walls) are designed according to the code recommendations. Then, the nonlinear model of the systems is prepared using fiber elements for the reinforced concrete wall and appropriate elements for the BRBs. Seismic responses of the combined systems subjected to ground motions at maximum considered earthquake level are investigated and compared to those obtained from BRBFs. Results showed that the maximum residual inter-story drift from the combined systems is, on average, less than half of the corresponding value of the BRBFs. In this research, mean of absolute values of the maximum inter-story drift ratio demand obtained from combined systems is less than the 3% limitation, while this criterion has not been fulfilled by BRBF systems.

**Keywords:** seismic response, Buckling-Restrained Braced Frames; reinforced concrete shear wall; earthquake records; combined system, frame

## 1. Introduction

Reinforced concrete (RC) shear walls and buckling-restrained braces (BRBs) are considered as two effective structural elements to resist seismic loads in mid- and high-rise structures. The seismic performance of concentrically buckling-restrained braced frames (BRBFs) has attracted the attention of many researchers and engineers. BRBs have the capability to prevent brace buckling in compression compared to conventional steel braces. They are designed to yield and dissipate energy during both tension and compression (Abdollahzadeh *et al.* 2013; Black *et al.* 2002; Aiken *et al.* 2002; Inoue *et al.* 2001; Eskandari and Vafaei, 2015; Eskandari *et al.*, 2017; Vafaei and Eskandari, 2014; Beiraghi 2018a,b). In conventional steel braces, due to buckling of the braces under compression, compressive strength of steel cannot be used efficiently and the hysteretic behavior of braces deteriorates severely under strong ground motions. In BRBs, the main concept is to confine a steel core element so that it can yield under compression as well as tension. In BRBs, concrete-filled steel tubes are used as confining mechanisms, while significant energy dissipation and ductility are demonstrated by experiments (Watanabe *et al.* 1988, Watanabe 1992). In one of the first studies, Tremblay *et al.* (1999) tested BRBs in support of a seismic retrofit project in Canada. Furthermore, viable all-steel BRBs have been developed more recently by researchers (Tremblay *et al.* 2006,

Wu *et al.* 2012, Judd *et al.* 2015).

In order to determine the seismic performance of structures with different configurations, several large-scale BRBFs have been examined by experimental and numerical tests. (Fahnestock *et al.* 2007a, Uriz and Mahin 2008, Tsai *et al.* 2008, Tsai and Hsiao 2008, Palmer *et al.* 2014, Tera'n-Gilmore *et al.* 2011, Guneyisi 2014). such tests identified the advantages of BRBs -i.e. ductility and energy dissipation capability- up to and beyond the expected design-level earthquake demands. Also, they demonstrated the potential deficiency of BRBFs, regarding the residual drift (NIST 2015). Numerous researchers have studied the range of drift and BRB deformation demands in BRBFs, including BRBF with moment-resisting frames, designed according to authentic codes (Sabelli 2001, Sabelli *et al.* 2003, Kiggins and Uang 2006, Uriz and Mahin 2008, Ariyaratana and Fahnestock 2011, Erochko *et al.* 2011). Compared with conventional CBF structures, BRBFs have lower initial and post-yield stiffness and therefore may be more sensitive to the formation of story mechanisms. In multiple stories, it would be desirable to achieve yield distribution (NIST 2015). In BRBFs, concentration of drift in one story may happen, as BRB yield in a given story can lead to significant reduction in stiffness of that story. This drift concentration is unpleasant and can lead to global instability caused by P-Delta effects. It may also lead to undesirable and significant residual drift. A proper solution to the issue has not been found yet. A double-stage yield buckling restrained brace has been proposed to prevent soft story collapse in structures subjected to strong earthquakes (Pan *et al.* 2017). Flogeras and Papagiannopoulos (2017) studied seismic responses from three-dimensional,

\*Corresponding author, Professor  
E-mail: [h.beiraghi@msh-iau.ac.ir](mailto:h.beiraghi@msh-iau.ac.ir)

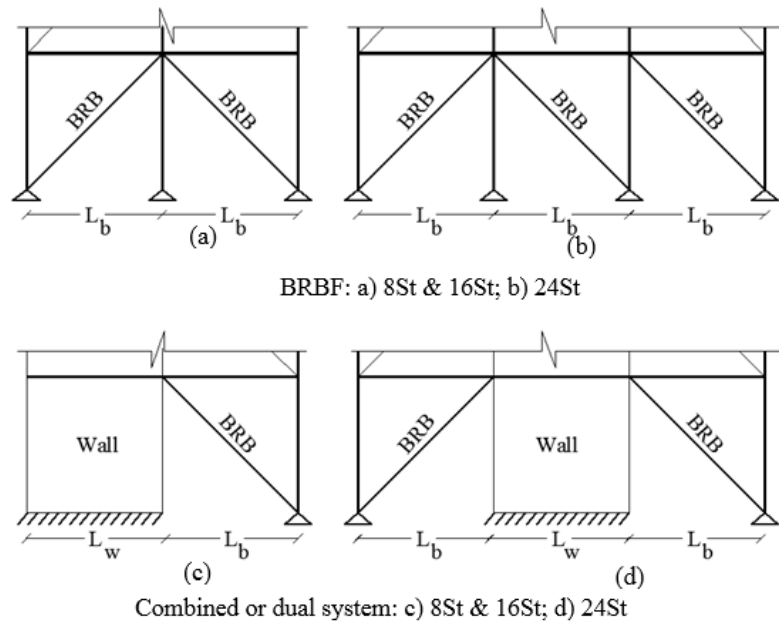


Fig. 1 General elevation of the assumed frames

nonlinear inelastic time-history analyses of some steel BRBFs, taking into account soil-structure interaction.

RC wall structures are well-known, lateral load-resisting systems used for rather tall buildings. Generally, they have acceptable stiffness and strength (Akbarzadeh *et al.* 2016). But during strong ground motions, in a cantilever tall RC wall, severe plasticity can extend to upper stories, so that intense damage occurs in those regions. This issue occurs due to higher-modes of vibration effects in a multi-story cantilevered RC wall (Panagiotou *et al.* 2009). Furthermore, shear wall-frame structural system in tall buildings under seismic analysis has been investigated (Park *et al.* 2014). To the knowledge of the author, the combination effect of RC wall and BRBF has not been studied previously. Enhancement is possible in the seismic performance of BRBFs, through combination with RC wall systems.

In this paper, BRBFs adjacent to special RC shear walls are used as a combined or dual system. This new system configuration consists of a reinforced concrete shear wall as well as BRBs, in order to resist the lateral loads and compensate for the shortcomings of the BRBFs. Some prototype models of the proposed systems with steel BRBF-only systems (without wall) are designed according to the code recommendations. Then, the nonlinear model of the systems is prepared and NLTHA is implemented. Combined system responses are investigated and compared with those obtained from BRBFs. Generally, the combined system functions better than the BRBF.

## 2. Design procedure

Structures of the case-study are 8, 16 and 24-story buildings with a typical floor height of 3.5 m. In the combined systems, RC wall along with BRBs resisted the whole seismic loads of ground motion for these buildings. In the BRBFs, BRBs resisted the whole seismic loads of

ground motion. Figure 1 shows the general view of the assumed frames. The cases are plane structures and the columns and beams are steel materials. The nominal design yielding stress of the reinforcement bar and steel material of the columns or beams are 400 and 370 MPa, respectively. The nominal strength of concrete is assumed to be 45 MPa.

ETABS software version 13.1.1 is used to design the assumed structures and create a linear elastic finite element model. Shell-type plate element is used to model the wall. This type of element uses a triangular or quadrilateral formulation that combines separate membranes and plate-bending behaviors. Line elements are used to create beams and columns. Connection between the beams and columns is of the pinned type. Wall bases are fixed and column bases are pinned. A general view of finite element models is shown in the following section. The portions for the dead and live load carried by the wall and columns are assigned to the wall. The appropriate mass portion of each story is assigned to mass center of the frame. A strength based design procedure is used and the design of frames is based on ASCE-7 and ACI318-11 (ACI 318, 2011; ASCE 7, 2010).

The heights of the examined systems are 28, 56 and 84 m. Characteristics of the designed frames are shown in Tables 1, 2 and 3.  $L_b$  and  $L_w$  are the widths of the braced bay and wall, respectively.  $P/A_g f_c$  is the axial force to cross-section area multiplied by concrete nominal strength ratio. Thickness of the wall is constant along the height and the specifications of BRB are identical at every 0.25H. Vertical steel reinforcement distribution is uniform at each section. The value of longitudinal reinforcement is determined so that the nominal flexural strength at each level is greater than that of the design envelope. The amount of reinforcement is considered invariable for every 25% height from the base. The calculated reinforcement ratio is shown in Table 3. The minimum reinforcement ratio is 0.25% (ASCE 7, 2010).

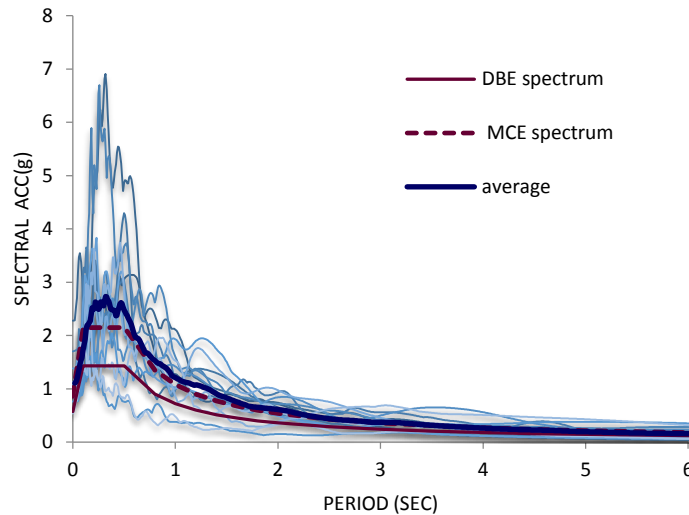


Fig. 2 Mean linear acceleration response spectra of the records, scaled to the maximum considered earthquake (MCE); DBE level spectrum and MCE level spectrum

Table 1 Geometry specification of the structures

		8ST	16ST	24ST
Total Height	H	28	56	84
BRBF	$L_b$	3.5	5	6.66
	$L_b$	3.5	3.5	7
Dual	$L_w$	2.5	5	6
	wall thickness	0.45	0.55	0.7

Table 2 General specifications of the designed structures

		8ST		16ST		24ST	
		BRBF	Dual	BRBF	Dual	BRBF	Dual
T	$T_1$	1.4	1.08	2.64	2.35	4	3.34
	$T_2$	0.495	0.3	0.7	0.63	1.22	0.9
	$T_3$	0.281	0.13	0.38	0.28	0.66	0.45
Seismic weight	W (Ton)	780	780	2870	3091	19800	
	$P/A_g f'_c$	-	3.7	-	5.1	-	
	$V_t/W$ %	8.2	11.3	6	6.6	4.2	
	$R_{eff}$	5.2	5	5.1	4.8	4.3	

In order to take the effect of cracks on wall stiffness into account, reduction factors for flexural stiffness are applied. A coefficient of 0.5 is used for the effective moment of inertia of the RC wall cross-sections. This coefficient is in accordance with the stiffness reduction factors recommended in ACI 318-11 (Sections 8.8 and 10.10).

The natural periods, mode shapes and modal mass participation factors are determined using the RSA procedure. More than 97% of the modal participation mass ratio resulted from the first five translational modes of vibration. A 5% damping DBE level response spectrum is used in the RSA procedure (see Figure 2). Response modification factor of the examined combined system is not evident, but that quantity is 8 for steel buckling-restrained braced frames as well as dual systems with special moment

frames and steel buckling-restrained braced frames (ASCE 7-2010). For both considered BRBF and combined (dual) systems, a response modification factor equal to eight ( $R=8$ ) seemed an appropriate option, used to obtain the design demand from an equivalent static procedure. The base shear force resulted from elastic RSA,  $V_t$ , is modified so that its quantity equaled 0.85 times the design equivalent static base shear force,  $V$ . ASCE 7 requires the forces to be multiplied by 0.85  $V/V_t$  (ASCE 7, 2010) when reduced combined base shear demand from modal responses (by dividing by a design  $R$  factor),  $V_t$ , is less than 85% design equivalent static base shear force ( $V$ ). This requirement controlled all the designed models; therefore, effective response modification factor in the RSA procedure,  $R_{eff}$ , is less than 8 (Table 2). In all models, the drift limit of the code governed the design.

BRB design conformed to the current prescriptive codes. To determine the size of the BRB braces, axial forces calculated from the modal response spectrum analysis are reduced by the value of the response modification factor. The capacity of braces under tension and compression are considered as  $\phi A F_y$ , where  $A$  is the cross section of brace element,  $\phi = 0.9$  and  $F_y = 250$  MPa (Sahoo *et al.* 2010).

According to AISC Seismic Provisions for Structural Steel Buildings (AISC 2010), columns in buckling restrained braced frames require to be checked primarily for the axial force and moment interaction for code level forces, and secondarily for the maximum axial load from the sum of the vertical components of all buckling restrained braces applied to the column along with tributary gravity loads. For the columns of assumed models, the second criterion governed the design and produced larger demand/capacity ratios.

BRBs have the capability of combined isotropic and kinematic hardening. They are rather stronger in compression than in tension. The reason is the Poisson expansion effect and friction at the interface between the core and the restraining material. According to the AISC

Table 3 Designed sections of the structures

	8ST		16ST		24ST		
	BRBF	Dual	BRBF	Dual	BRBF	Dual	
Longitudinal reinforcement ratio (%)	0-25%H	-	2	-	2	-	1.85
	25-50%H	-	0.97	-	1.01	-	0.32
	50-75%H	-	0.72	-	0.9	-	0.38
	75-100%H	-	0.35	-	0.54	-	0.37
Cross-section area of BRB yielding core (cm <sup>2</sup> )	0-25%H	45	45	87	100	220	220
	25-50%H	32	45	74	84	200	190
	50-75%H	26	35	58	52	142	135
	75-100%H	19	19	45	45	132	116
Cross-section area of column section (cm <sup>2</sup> )	0-25%H	288	288	650	650	2352	1390
	25-50%H	204	204	440	440	1390	1260
	50-75%H	105	105	250	250	1100	1100
	75-100%H	47	47	110	90	360	300
Beam Type	W6X12	W6X12	W8X31	W8X31	W12X65	W12X65	

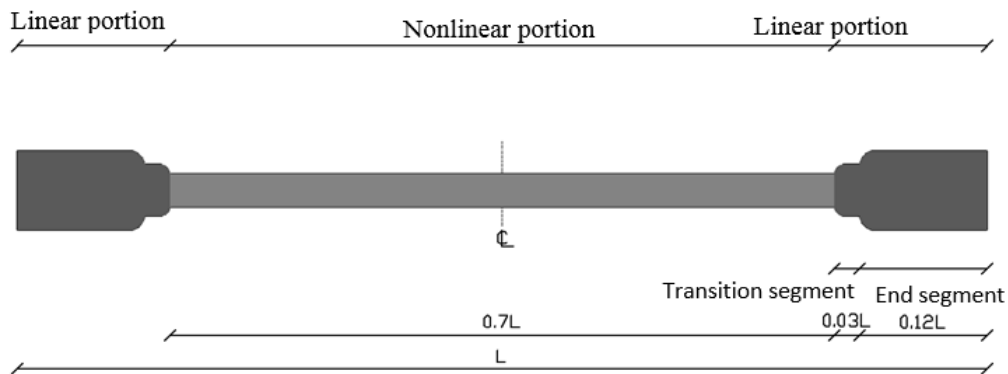


Fig. 3 Buckling restrained brace segments

Seismic Provisions, the seismic behavior of BRBs including strain hardening is accounted for the compression strength and the strain hardening adjustment factors. Thus, the maximum compression forces from the brace are calculated as  $R_y \omega \beta A F_y$ , where  $R_y = 1.1$  accounts for the material over strength,  $\omega = 1.25$  represents the strain-hardening effect and  $\beta = 1.1$  is the compression over-strength factor (Jones *et al.* 2013).

### 3. Nonlinear modeling

To investigate the seismic behavior of structures, nonlinear models are made in Perform-3D software (PERFORM-3D 2011). The columns and beams are modeled by elastic elements. After each analysis, the elastic behavior of these elements is checked via controlling the demand/capacity ratio. The corresponding mass quantity is assigned to the center of mass at each frame floor.

#### 3.1 BRB Behavior

BRB element in Perform-3D is a bar-type component that only resists axial force and has no resistance to torsional or bending forces (PERFORM-3D User guide 2006). The element contains two bars in series. There is a linear portion that is elastic and a nonlinear core portion capable of yielding.

The length of restrained nonlinear core portion of a BRB element is assumed to be 0.7 times as much as the node-to-node brace element length. The remaining 30% is considered as the linear non-yielding portion. This linear portion of the brace accounts for the stiffness of the gusset, the brace connection, and the portion of the column, not considered in center-line to center-line geometry. Typically, the linear portion consists of the transition and end segments (Figure 3). To prevent the yielding of transition and end segments, cross section area of these segments are considered larger than the restrained nonlinear core portion. In this study, the cross section area of transition and end segments ( $A_t$  and  $A_e$ ) of the BRB elements are chosen as 1.6 and 2.2 times the area of the core cross-section, respectively. Besides, the length of the transition and end segments are chosen as 0.06 and 0.24 times the total length of the bracing, respectively (Nguyen *et al.* 2010). To calculate the cross section area of the nonlinear core ( $A_c$ ) of the BRB element, the following equation is used (Bosco *et al.* 2010)

$$\frac{L_c}{A_c} = \frac{L_w}{A} - \frac{L_e}{A_e} - \frac{L_t}{A_t} \quad (1)$$

Where  $L_c$ ,  $L_t$ ,  $L_e$  and  $L_w$  represent the lengths of the yielding core, transition segment, end segment and the whole bracing respectively; and  $A$  is the cross-section area of the equivalent bar calculated from the elastic design procedure. Figure 4 shows the backbone curve for the BRB element used in nonlinear model (Simpson *et al.* 2009).

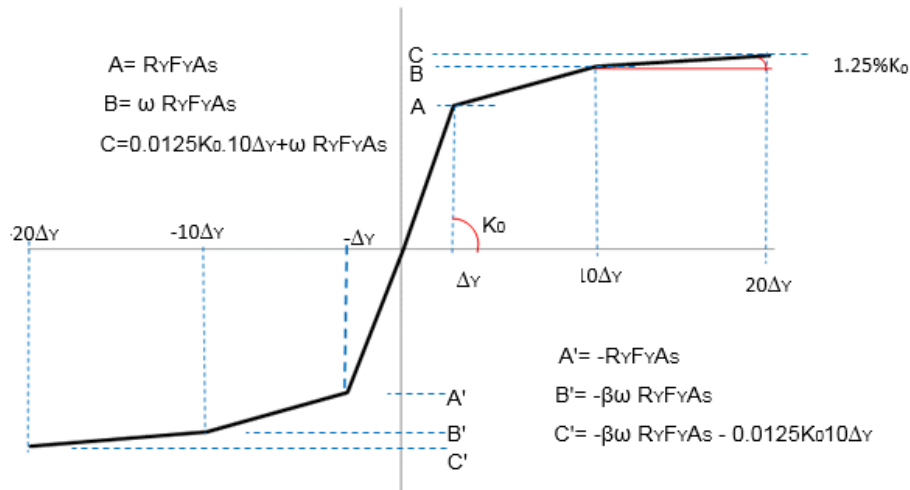


Fig. 4 Backbone curve for the BRB element (Simpson, Gumpertz, Heger, Inc, 2009).

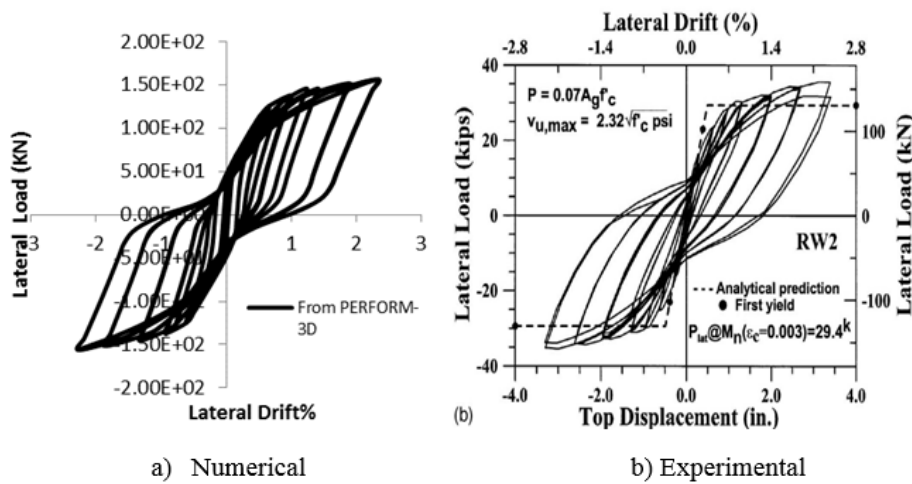


Fig. 5 Comparison of hysteresis loops from: (a) numerical from software and (b) experimental results (Orakcal *et al.* 2006)

### 3.2 Software verification

Some researchers have demonstrated the capability of fiber element models to simulate the behavior of RC shear walls (Beiraghi *et al.* 2016; Orakcal and Wallace, 2006). Generally, fiber element models are preferred over the lumped-plasticity beam–columns. Fiber element models can predict the neutral axis migration within the RC concrete walls subject to lateral loads. (Applied Technology Council, 2010). Fiber wall elements consider distinct longitudinal (vertical) and transverse directions: Axis-2 is vertical, Axis-3 horizontal, and Axis-1 normal to the wall plane. For thin RC walls, using one element for each story has enough accuracy (PERFORM-3D, 2006). In the vertical direction, the fibers of a wall element could yield to bending. Besides, transverse in-plane behavior and out-of-plane bending are essentially elastic and secondary (PERFORM-3D, 2006).

An Experimental test data on a slender RC shear wall subjected to cyclic lateral loading is used to verify the accuracy of the fiber wall elements. (Thomsen and Wallace, 2004). In the test program, capacity design is used to design this specimen to allow for flexural hinging at the

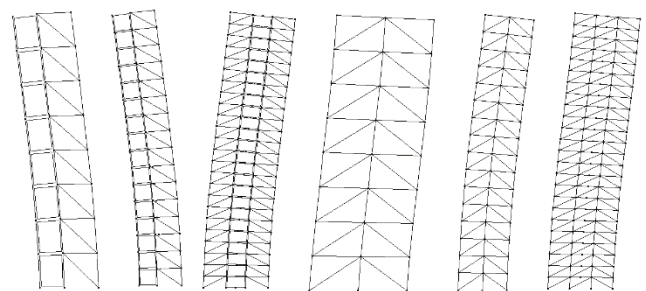


Fig. 6 The elevation view of the nonlinear structural models for the combined (dual) systems and BRBFs at first mode of vibration

base. In the numerical model, five nonlinear shear wall elements over the height and eight vertical concrete and eight vertical steel fibers are used in each element. Inelastic strain tends to concentrate on a single element at the base. Therefore, an element length equal to the assumed plastic hinge length of  $0.5L_w$  is used, where  $L_w$  is the wall length (ASCE/SEI 41-13, 2014). The graph of lateral load versus top drift is relatively insensitive to the mesh size and

Table 4 List of ground motion records used to carry out NLTHA

Event name	PEER code*	Year	Record duration (s)	Station	PGA*	PGV*	M
Northridge	960	1994	20	Canyon Country-WLC	0.48	45	6.7
Duzce	1602	1999	56	Bolu	0.82	0.62	7.1
Hector Mine	1787	1999	45.3	Hector	0.34	42	7.1
Imperial valley	169	1979	100	Delta	0.35	33	6.5
Imperial valley	174	1979	39	El centro Array#11	0.38	42	6.5
Kobe, Japan	1116	1995	41	Shin- Osaka	0.24	38	6.9
Kocaeli, Turkey	1158	1999	27.2	Duzce	0.36	59	7.5
Kocaeli, Turkey	1148	1999	30	Arcelik	0.22	40	7.5
Landers	900	1992	44	Yermo Fire Station	0.24	52	7.3
Loma Prieta	767	1989	40	Gilroy Array	0.56	45	6.9
Superstition Hills	721	1987	40	El Centro Imp. Co.	0.36	46	6.5
Superstition Hills	725	1987	22.3	Poe Road (temp)	0.45	36	6.5
Chi chi, Taiwan	1244	1999	90	Chy101	0.44	115	7.6
San Fernando	68	1971	28	LA-Hollywood Stor	0.21	19	6.6

\* Pacific Earthquake Engineering Research Center Strong Motion Database

\* PGA: Peak ground acceleration

\* PGV: Peak ground velocity

number of fibers. Cyclic lateral displacement is applied at the top of the wall. Figure 5 compares the results of numerical and experimental hysteresis loops. The horizontal axis is the lateral drift at top of the specimen. A good compromise is observed in the results.

In the case under study, shear wall elements are used to model RC walls. Each fiber cross section is comprised of the vertical steel and concrete fibers. For nonlinear fiber model of the wall, a confined concrete stress-strain based on the modified Mander model is assumed (Mander *et al.* 1988). Tensile strength of the concrete is ignored. The expected yield strength of the steel reinforcement is 1.17 times its nominal yield strength and the expected concrete fiber compressive strength is 1.3 times the specified strength used in the design procedure (LATBSDC, 2011). Strength and stiffness degradation factors are applied to specify the degradation factor for longitudinal reinforcements. This factor represents the ratio of the areas of the degraded to non-degraded hysteresis loops (Ghodsi *et al.* 2010). One element for each story is used to model the RC wall at the first floor.

To monitor the compressive strain at the critical sections, the effective plastic hinge length is used at the base of the wall models. For analyses purposes, the plastic-hinge length ( $l_p$ ) in the RC walls can be calculated from the following formula given by Paulay and Priestley (1992)

$$l_p = 0.2L_w + 0.03h \quad (2)$$

Where  $L_w$  is the RC wall length and  $h$  is the wall height. The height of the finite element used to model the plastic hinge shall not exceed the length,  $l_p$ , or the story

height at the location of the critical section (LATBSDC, 2011).

Figure 6 represents the elevation view of the 6 nonlinear structural models. Linear shear model is assumed in the RC wall models. A typical value for the shear stiffness of the wall models is  $G_c A_g / 10$  to  $G_c A_g / 20$  as recommended by ATC72 (Applied Technology Council, 2010). In the current research,  $G_c A_g / 15$  is used, where  $G_c A_g$  is the elastic shear stiffness.

### 3.4 Damping consideration

PERFORM-3D software has the ability to take Rayleigh and modal damping into consideration. To obtain a realistic response of structures, selection of reasonable damping coefficient is necessary (Léger and Dussault, 1992). Chopra (2001) states that Rayleigh damping can only be used when relevant mechanisms are provided throughout the structure (Chopra, 2001). According to the software user guide, using a combination of modal and Rayleigh damping is a proper approach (PERFORM-3D, 2006). In this project, a small amount of Rayleigh damping is added to the regular modal damping to damp out high-frequency vibrations. 2.5% of the modal damping for all modes along with 0.2% Rayleigh damping for the first and third modes are used according to the software guideline (PERFORM-3D, 2006).

### 3.5 Strong Motion Records

An appropriate set of ground motion records is necessary to implement NLTHA. Maximum Considered

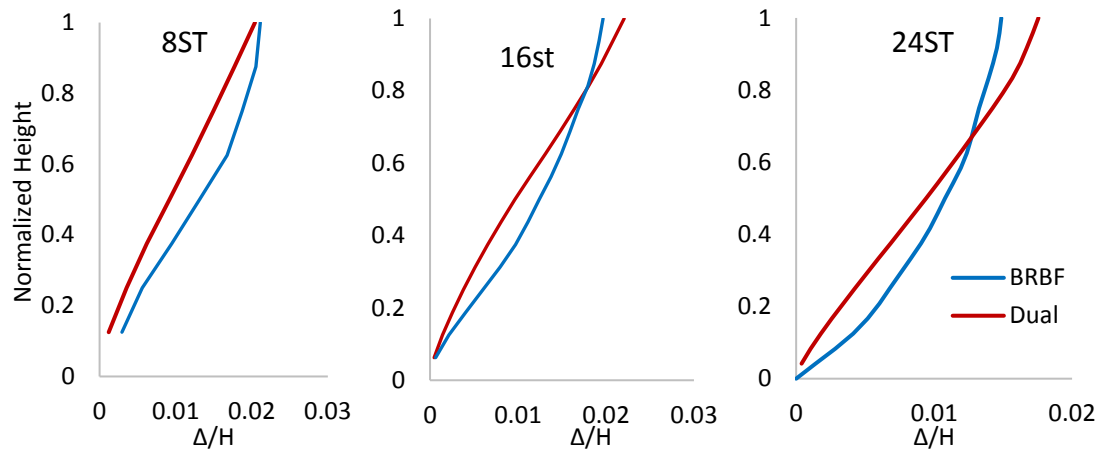


Fig. 7 Mean lateral displacement demand envelopes

Earthquake (MCE) level is used to evaluate the performance of the systems. According to the LATBCD, the structural responses must be calculated at MCE level. This level of evaluation is intended to demonstrate a low probability of collapse when the building is subjected to the MCE ground motions (LATBSDC, 2011). The response spectrum graph of the MCE level is 1.5-times the DBE response spectrum graph level (ASCE 7, 2010). A total of 14 horizontal far-field ground motions is selected from the pertinent set of FEMA P695 (2009). All records are fault normal components of the ground motions, and their time histories are obtained from the PEER NGA database. The ground motion characteristics are represented in Table 4. The scaling method is critical in the NLTHA and can essentially affect the results (Beiraghi *et al.* 2017). The scaling procedure of the records is completed as per ASCE7. The ground motions are linearly scaled such that their mean spectra for 5% damping ratio, matched or exceeded the MCE design spectrum over periods ranging from 0.2T to 1.5T, where T is the estimated building fundamental period (ASCE/SEI 7-2010, 2010). In the subsequent section, structural performance will be presented for buildings subjected to the earthquake motions.

#### 4. Nonlinear structural performance

Mean of the structures' lateral displacement demand envelopes subjected to the earthquake records is illustrated in Figure 7. The horizontal axes are normalized by dividing the lateral displacement by the total height of the building and the vertical axis is of normalized height. In the 8-story structure, roof displacement ratio of the BRBF and combined system are almost the same. However, in the 16- and 24-story buildings, the roof displacement demand of the combined system is larger than that of the BRBF. As discussed later in this paper, the upper part of the BRBFs has a smaller drift angle, compared with combined systems. Generally, the lower part displacement of the combined systems is less than the corresponding displacement of the BRBFs. In the combined system, the wall deformation mode tends to be in flexure, so the wall has less

displacement at the lower level of the structure. However, BRBF tends to have racking story deformation (shear deformation mode) that leads to larger drift angle demand at lower levels and less drift angle at the upper levels. In the combined system, the displacement inclination of the wall and BRBF are different and there are interactions between these lateral load bearing systems. It is worth mentioning that, the overall trends of the displacement curves are identical for the combined system and for BRBFs.

One of the most important responses of the structures is the maximum inter-story drift ratio (MIDR) parameter. Figure 8 shows the mean envelope of the MIDR demand for the 8-, 16- and 24-story buildings subjected to the selected records. Generally, in BRBF structures, MIDR occurs at the lower level of the system, while in the combined system, it occurs at the upper levels. The reason is the different deformation modes of BRBFs and RC walls. In BRBF structures, the variation of BRB section and its properties along the height, at every 0.25H, causes local rising in the MIDR demand at the corresponding levels. This issue can lead to story mechanism in the BRBFs subjected to severe earthquakes. Thanks to RC walls in combined systems, local rising in MIDR demand is slight. The presence of RC walls reduces MIDR, especially in short structures. On average, MIDR calculated in combined systems is less than 0.8 times the corresponding values obtained from BRBF structures. According to LATBCD, in each story, the mean of absolute values of MIDR from a suite of analyses shall not exceed 3% (LATBSDC, 2011). In this research, the mentioned demand for all examined combined systems is less than the 3% limitation. For BRBF-only systems, this demand is 4.2, 3.5 and 2.8% for 8-, 16- and 24-story structures.

Figure 9 indicates the average curvature ductility demand envelope of the RC wall in the 8-, 16- and 24-story combined systems. Curvature ductility demand represents plasticity extension in the RC wall. The rotation over each wall element is calculated using rotation gauge elements in Perform-3D computer program and the approximate curvature is calculated by dividing the rotation by the element height. The yield curvature,  $\Phi_y$ , is calculated from Equation (3) below, proposed by Paulay for rectangular RC walls (Paulay *et al.* 1992).

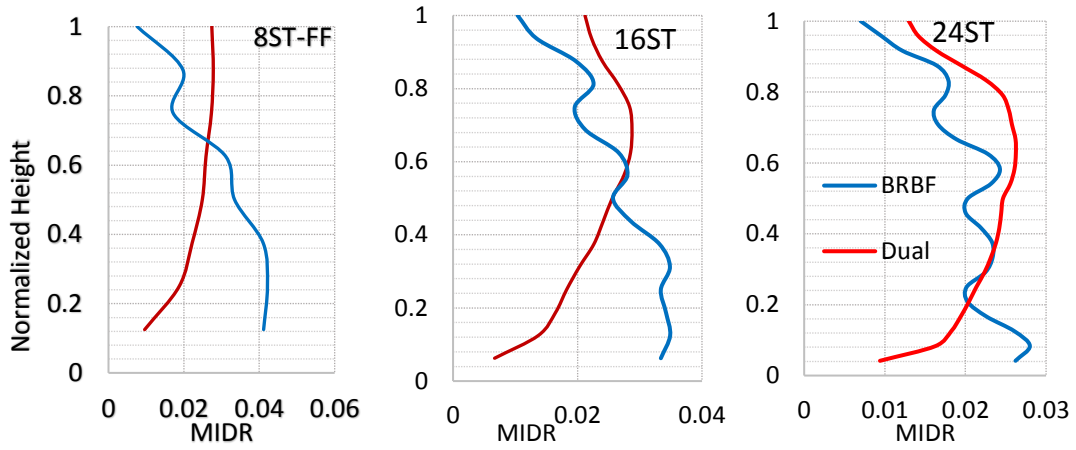


Fig. 8 Mean maximum inter-story drift ratio demand envelopes

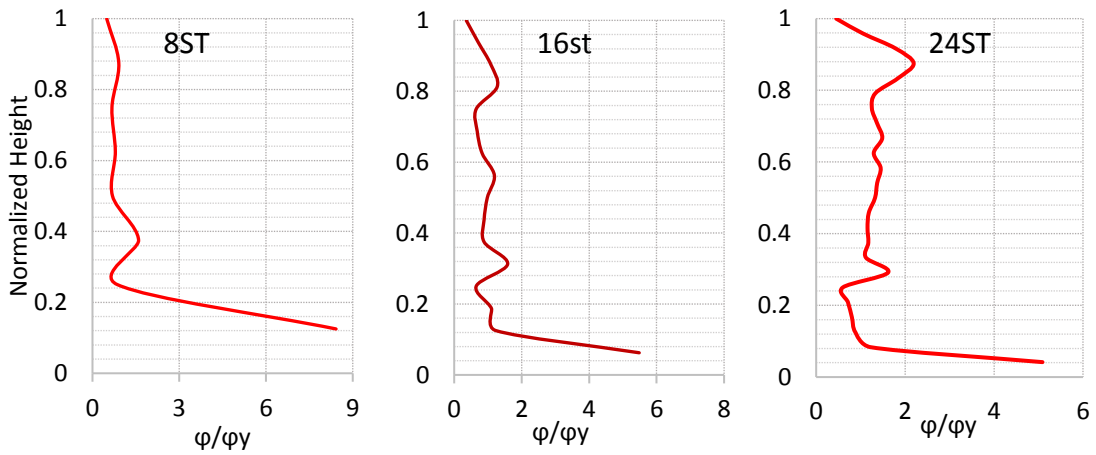


Fig. 9 Mean curvature ductility demand envelopes pertaining to the RC walls in the combined systems

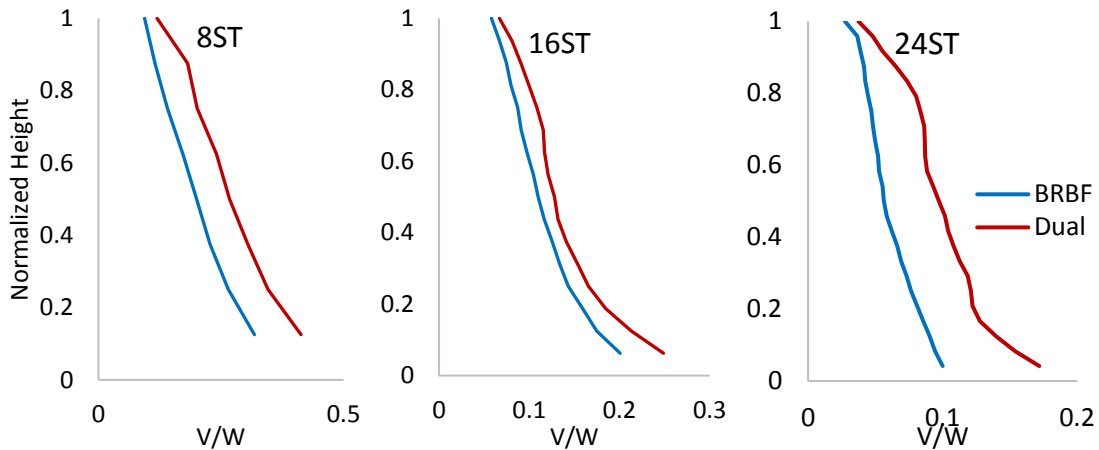


Fig. 10 Mean story shear demand envelopes

$$\Phi_y = \frac{1.8\epsilon_y}{L_w} \tag{3}$$

Where  $\epsilon_y$  is the expected yield strain of steel bars equal to 0.00234 and  $L_w$  is the wall length. To calculate the RC wall curvature ductility ( $\mu$ ), the following formula is used

$$\mu = \Phi/\Phi_y \tag{4}$$

Where  $\Phi$  is the mean measured curvature demand in one wall element. It is assumed that the demand curvature is constant along an element. According to the figure, the most curvature ductility demand is at the base of the RC walls. However, slight plasticity demand in some upper regions is also visible. In high RC wall-only structures in which the lateral force resistant system is just the RC wall, the plasticity extension in the upper region of the wall is critical (Beiraghi *et al.* 2018c, d), whereas in this study it is

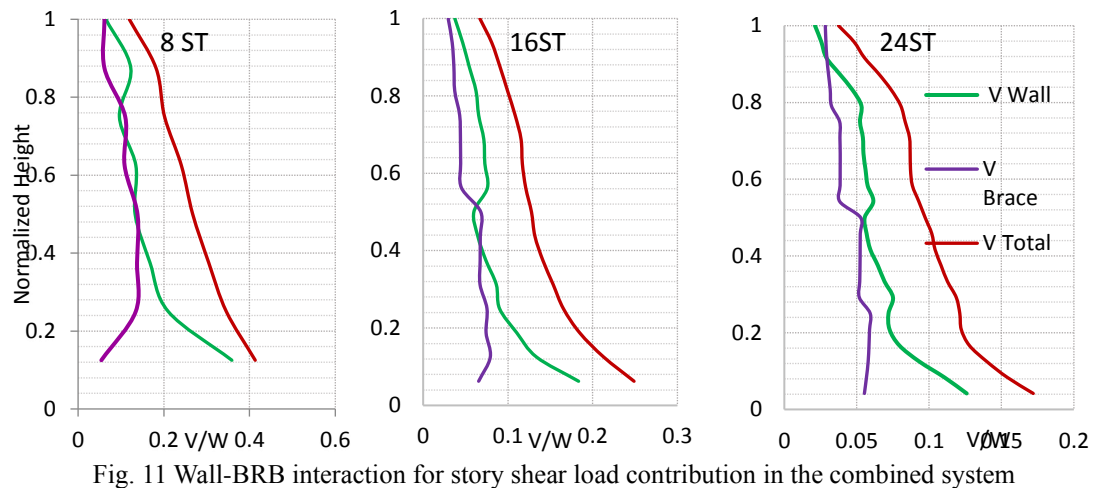


Fig. 11 Wall-BRB interaction for story shear load contribution in the combined system

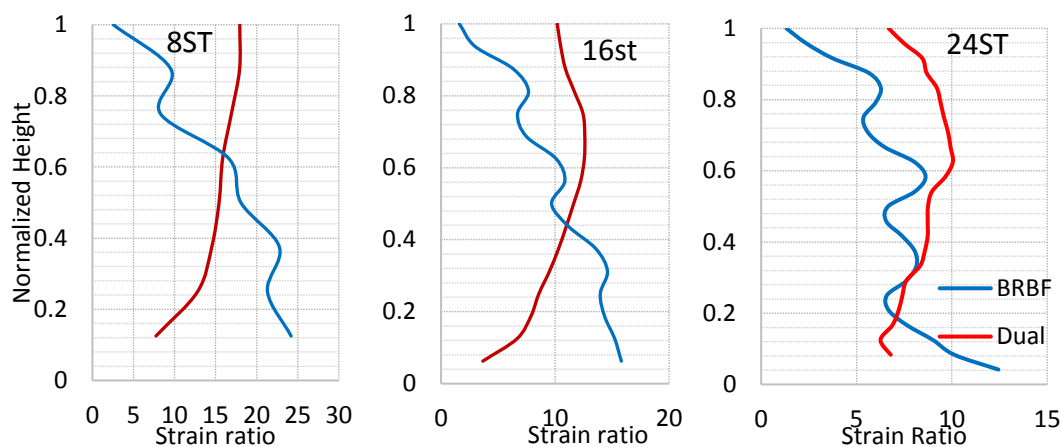


Fig. 12 Strain ratio envelopes (mean measured strain demand divided by the expected yielding strain) of the BRB core material

moderate because of the combination of the wall and BRBF like a dual system. Local rising occurs in the curvature ductility demand curve along the height of the structure because of the longitudinal reinforcement curtailment.

Mean shear demand envelopes of the systems subjected to earthquake events have been demonstrated in Figure 10. Shear demand in horizontal axis has been divided by the total seismic weight of the structure ( $W$ ) and the vertical axis is normalized height. As expected, the shear demand from combined system is larger than that of the BRBF system. The reason is the larger stiffness of the combined structures leading to smaller vibration periods and hence larger shear demand.

For the combined systems, Figure 11 represents the contribution of BRBs and the wall for bearing the mean lateral shear load along the height subjected to the earthquake records. It is obvious that in each level of the combined structures, the shear force is carried by the RC wall as well as BRBs. At the lower levels, the shear quota of the wall is larger than the BRBs. For example, the wall shear demand at the base of the 24-story building is more than twice as that of the BRBs. This ratio is larger for shorter structures. The reason is the greater stiffness and less lateral displacement of the wall compared to the BRBFs, especially at the lower levels of a system.

Commonly, in the lower levels, the racking deformation tendency of the BRBFs for the shorter structures is stronger than that for the taller ones; therefore, in shorter buildings, the difference between the shear load contribution of the wall and the BRBFs is more severe.

Figure 12 compares the mean envelope of strain ratio demand in the BRBs of BRBF and combined systems. The value of the horizontal axis is the mean measured strain demand divided by the expected yielding strain of the BRB core material. General trend of the BRB strain ratio demand curves along the height of the combined system is constant. The local rising in the strain ratio demand curve of BRBF structure is because of the variation in the BRB properties, every  $0.25H$ . Typically, in the BRBF systems, the maximum strain ratio of BRB occurs at the lower levels, reversing in the combined systems. In each case of the BRB strain demand curves, the usual trend is similar to the MIDR demand. For both BRBF and combined systems, the higher the building, the smaller the maximum BRB strain. For example, in the BRBFs, for 8-, 16-, 24-story structures, the maximum BRB strain ratios are 23, 15 and 12.5, respectively. Whereas in the combined systems, these values will be 16, 12 and 10. On average, the maximum strain ratio of the BRBs in the BRBFs is 1.25 times the corresponding value in the combined systems. It is worth

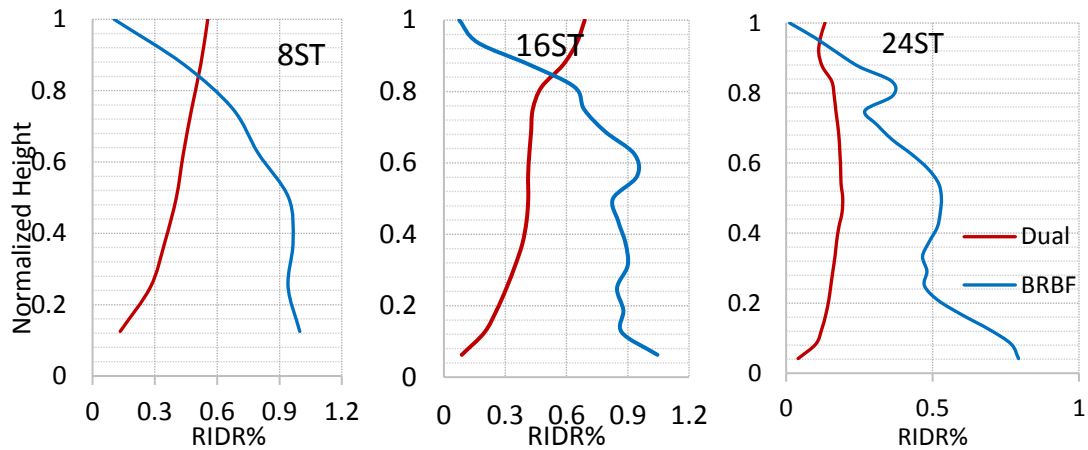


Fig. 13 The mean residual IDR demand envelope

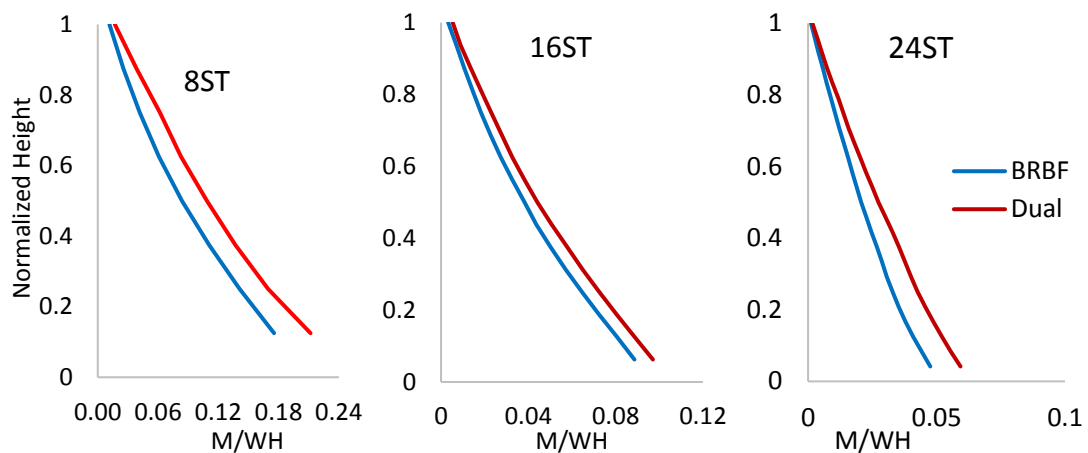


Fig. 14 Mean story overturning moment demand envelopes

mentioning that the acceptance criterion for the strain ratio of the BRBs, according to ASCE 41-13, is 13.3.

Residual drift of the BRBF systems subjected to seismic forces is one of the most recognized deficiencies of these systems. According to LATBCD, the mean absolute demand of residual IDR (RIDR) from a suite of analyses shall not exceed 1%. The mean residual IDR demand envelope of the studied structures has been displayed in Figure 13. Commonly, the trend of the residual IDR for the BRBF system is different from the corresponding curve for the combined system. In all of the structures, the maximum residual IDR demand is less than the 1% limit. Furthermore, the maximum residual IDR demand from BRBF structure is considerably larger than the corresponding demand from combined structures. For instance, in the BRBFs, the maximum residual IDRs for 8-, 16-, 24-story structures are 0.94, 0.95 and 0.79%, respectively. These values in the combined systems are 0.55, 0.68 and 0.19%. Approximately, the mean maximum residual IDR from the combined systems is half of the corresponding values from BRBFs. From an economic viewpoint, scholars believe that the building should be rebuilt rather than repaired when maximum residual IDR exceeds 0.5% (McCormick *et al.* 2008).

The mean story overturning moment demand envelope along building height has been shown in Figure 14. The

moment envelopes have been normalized by the product of the total seismic weight and height of the buildings. Generally, the moment of the combined system is larger than that of the BRBF. This issue is in accordance with the shear demand envelope.

## 8. Conclusions

The seismic responses of combined structural systems (dual), consisting of BRBFs and Special RC shear walls are investigated in this paper. Proposed system compensates for the deficiencies of BRBFs. Some prototype models of the proposed combined systems as well as some steel BRBF-only systems (without wall) are designed according to the code recommendations. Then, nonlinear model of the systems is prepared using fiber elements for RC wall and appropriate elements for BRBs. Finally, NLTHA is implemented using the severe ground motion records at MCE level ground motions. Behavior of the combined systems is investigated and compared to that obtained from BRBF-only systems. The following results can be concluded:

- The results show that the maximum residual inter-story drift from the combined systems is on average less than half of the corresponding value from the BRBFs.

- Approximately, the mean maximum strain ratio of the BRBs in BRBFs is 1.25 times the corresponding value in the combined systems.

- In the lower part of the structures, lateral displacement of the combined systems is less than the corresponding displacement of the BRBF. The reason is the wall deformation mode that tends to be in flexure, so, the wall and consequently the combined system has more resistance to displacement at the lower level of the structure. BRBFs tend to shear deformation mode and therefore, in this structures, the MIDR occurs at the lower levels, while, in the combined system, this issue occurs at the upper levels.

- At the lower levels of the combined system, the story shear quota of the wall is considerably larger than the BRBs. Commonly, in the lower levels of the shorter structures, the racking deformation tendency of the BRBFs is stronger than that of the taller structures. Therefore, in the lower levels of the shorter combined buildings, the difference between the shear load contribution of the wall and the BRBs is more severe.

- In the BRBF structures, variation of the BRB section and its properties along the height, causes local rising in the MIDR demand curve at the corresponding levels. This issue can lead to story mechanism in the BRBFs systems subjected to sever ground motions, which does not appear in the combined system because of the RC wall existence.

- In the RC wall of combined system, plasticity extension is mostly at the base of the wall, in such a way that the curvature ductility at the wall base is less than 8 for all cases, that is deemed moderate. Plasticity extension in some upper regions of the RC wall is very slight, because of the combination of the wall and BRBF.

According to LATBCD, in each story, the mean of the absolute values of the MIDR from a suite of analyses shall not exceed 3%. In this research, the mentioned demand calculated from combined systems is less than the 3% limitation; while this criterion has not been fulfilled by 8- and 16-story BRBF systems. Eventually, it is concluded that the combined system is a generally more appropriate solution than BRBFs.

## References

- Aiken, I.D., Mahin, S.A. and Uriz, P. (2002), "Large-scale testing of buckling-restrained braced frames" Proc. Japan Passive Control Symposium, Tokyo Institute of Technology, Japan, 35-44.
- Ariyaratana, C.A. and Fahnestock, L.A. (2011), "Evaluation of buckling-restrained braced frame seismic performance considering reserve strength" *Engineering Structures*, 33, 77-89.
- ACI 318 (2011), Building code requirements for structural concrete and commentary. ACI Committee 318: Farmington Hills.
- AISC (2010), Seismic provision for structural steel buildings. American Institute of Steel Construction: Chicago.
- Applied Technology Council (2010), ATC-72: Modeling and Acceptance Criteria for Seismic Design and Analysis of Tall Buildings. ATC: Redwood City, CA.
- ASCE/SEI 7 (2010), Minimum design loads for buildings and other structures. American Society of Civil Engineers: Reston, VA.
- ASCE/SEI 41 (2014), Seismic rehabilitation of existing buildings (Including Supplement # 1). American Society of Civil Engineers: Reston, VA.
- Abdollahzadeh, G. and Banihashemi, M. (2013), "Response modification factor of dual moment-resistant frame with buckling restrained brace (BRB)", *Steel and Composite Structures*, 14(6), 621-636
- Akbarzadeh-Bengar, H. and Mohammadalipour Aski R. (2016), "Performance based evaluation of RC coupled shear wall system with steel coupling beam", *Steel and Composite Structures*, 20(2), 337-355
- Beiraghi H, Siahpolo N. 2016. Seismic assessment of RC core-wall building capable of three plastic hinges with outrigger The *Structural Design of Tall and Special Buildings*. 26(2):e1306.
- Beiraghi H, 2017. Earthquake effects on the energy demand of tall reinforced concrete walls with buckling-restrained brace outriggers. *Structural Engineering and Mechanics*. 63(4):521-536.
- Beiraghi H, 2018a. Energy Dissipation of Reinforced Concrete Wall Combined with Buckling-Restrained Braces Subjected to Near- and Far-Fault Earthquakes Iran J Sci Technol Trans Civ Eng 42(4): 345-359
- Beiraghi H, 2018b. Energy demands in reinforced concrete wall piers coupled by buckling restrained braces subjected to near-fault earthquake. *Steel and Composite Structures*. 27(6): 703-716
- Beiraghi H, 2018c. Reinforced concrete core-walls connected by a bridge with buckling restrained braces subjected to seismic loads. *Earthquakes and Structures*. 15(2): 203-214
- Beiraghi H, 2018d. Near-fault ground motion effects on the responses of tall reinforced concrete walls with buckling-restrained brace outriggers. *Scientia Iranica A* 25(4), 1987-1999
- Bosco, M. and Marino E.M. (2013), "Design method and behavior factor for steel frames with buckling restrained braces", *EARTHQUAKE ENGINEERING & STRUCTURAL DYNAMICS*, 42, 1243-1263. DOI: 10.1002/eqe.2269.
- Black, C., Makris, N. and Aiken, I. (2002), "Component testing, stability analysis and characterization of buckling-restrained braces", Report No. PEER-2002/08, Pacific Earthquake Engineering Research Center, University of California, Berkeley, CA, USA.
- Chopra, AK. (2001), *Dynamics of structures*. Prentice-Hall: New Jersey.
- Eskandari, R. and Vafaei, D. (2015) "Effects of near-fault records characteristics on seismic performance of eccentrically braced frames," *Structural Engineering and Mechanics* 56(5):855-870.
- Eskandari, R., Vafaei, D., Vafaei, J. and Shemshadian ME. (2017) "Nonlinear static and dynamic behavior of reinforced concrete steel-braced frames," *Earthquakes and Structures* 12(2):191-200.
- Erochko, J., Christopoulos, C., Tremblay, R. and Choi, H. (2011), "Residual drift response of SMRFs and BRB Frames in steel buildings designed according to ASCE 7-05", *Journal of Structural Engineering*, 137 (5), 589-599.
- FEMA P695 (2009), Quantification of Building Seismic Performance Factors (ATC-63 Project). Federal Emergency Management Agency, Washington D.C.
- Fahnestock, L. A., Ricles, J. M., and Sause, R. (2007a), "Experimental evaluation of a large-scale buckling-restrained braced frame", *Journal of Structural Engineering*, 133 (9), 1205-1214.
- Flogeras, A. K. and Papagiannopoulos, G. A. (2017), "On the seismic response of steel buckling-restrained braced structures including soil-structure interaction", *Earthquakes and Structures*, 12(4), 469-478.
- Guneyisi, E. M., Ameen N. (2014), "Structural behavior of conventional and buckling restrained braced frames subjected to near-field ground motions" *Earthquakes and Structures*, 7(4): 553-570.
- Ghodsii, T., Ruiz J.F., Massie C. and Chen Y. (2010), "Pacific earthquake engineering research/seismic safety commission tall

- building design case study”, *The Structural Design of Tall and Special Buildings* 19(2), 197–256.
- Inoue, K., Sawaisumi, S., and Higashibata, Y. (2001), “Stiffening requirements for unbonded braces encased in concrete panels”, *ASCE J. Struct. Eng.*, 127(6), 712–719.
- Jones, P. and Zareian F. (2013), “Seismic response of a 40-storey buckling-restrained braced frame designed for the Los Angeles region”, *The Structural Design of Tall and Special Buildings*, 22 (3), 291–299. DOI: 10.1002/ta1.687.
- Judd, J., Phillips A., Eatherton M., Charney F., Marinovic I. and Hyder C. (2015), “Subassemblage testing of all-steel web-restrained braces”, *STESSA*, Shanghai, China.
- Kiggins, S., and Uang, C. M. (2006), “Reducing residual drift of buckling-restrained braced frames as a dual system”, *Engineering Structures*, 28, 1525–1532.
- Léger, P. and Dussault S. (1992), “Seismic-energy dissipation in MDOF structures”, *Journal of Structural Engineering* 118(5), 1251–1269.
- LATBSDC (2011), *An Alternative Procedure For Seismic Analysis and Design of Tall Buildings Located in the Los Angeles Region*. Los Angeles Tall Buildings Structural Design Council: Los Angeles.
- Mander, J.B., Priestley M.J.N. and Park R. (1988), “Theoretical stress-strain model for confined concrete”, *ASCE Journal of Structural Engineering* 114(8), 1804–1826.
- McCormick, J., Aburano, H., Ikenaga, M. and Nakashima, M. (2008), “Permissible residual deformation levels for building structures considering both safety and human elements”, *Proc. 14th World Conference Earthquake Engineering*, Paper No. 05-06-0071, Beijing, China.
- NIST (2015), *Seismic design of steel buckling-restrained braced frames: A guide for practicing engineers*, GCR 15-917-34, NEHRP Seismic Design Technical Brief No. 11, produced by the Applied Technology Council and the Consortium of Universities for Research in Earthquake Engineering for the National Institute of Standards and Technology, Gaithersburg, MD.
- Nguyen, A.H., Chintanapakdee C. and Hayashikawa T. (2010), “Assessment of current nonlinear static procedures for seismic evaluation of BRBF buildings”, *Journal of Constructional Steel Research*, 66(8-9), 1118–1127.
- Orakcal, K., Wallace J.W. (2006), “Flexural modeling of reinforced concrete walls-experimental verification”, *ACI Structural Journal* 103(2), 196–206.
- Pan, P., Li W., Nie X. and Deng K, Sun J. (2017), “Seismic performance of a reinforced concrete frame equipped with a double-stage yield buckling restrained brace”, *The Structural Design of Tall and Special Buildings*. 26(4), e1335
- Park, Y., Kim H. and Lee D. (2014), “Efficient structural analysis of wall-frame structures”, *The Structural Design of Tall and Special Buildings* 23(10), 740–759
- Paulay, T. and M. J. N. Priestley (1992), “*Seismic Design of Reinforced Concrete and Masonry Buildings*”, John Wiley and Sons, New York.
- Palmer, K. D., Christopoulos, A. S., Lehman, D. E., and Roeder, C. W. (2014), “Experimental evaluation of cyclically loaded, large-scale, planar and 3-d buckling-restrained braced frames”, *Journal of Constructional Steel Research*, 101, 415–425.
- Panagiotou, M. and Restrepo J. (2009), “Dual-plastic hinge design concept for reducing higher-mode effects on high-rise cantilever wall buildings”, *Earthquake Engineering and Structural Dynamics*. 38, 1359–1380.
- PERFORM-3D (2011), *Nonlinear Analysis and Performance Assessment for 3D Structures*, V.4.0.3. Computers and Structures, Inc., Berkeley, CA.
- PERFORM-3D (2006), “*Nonlinear Analysis and Performance Assessment for 3D Structures*”, V.4, User Guide. Computers and Structures, Inc., Berkeley, CA.
- Sahoo, DR. and Chao S. (2010), “Performance-based plastic design method for buckling-restrained braced frames”, *Engineering Structures*, 32, 2950–2958.
- Simpson, Gumpertz, & Heger, Inc. (2009), “*Detailed Design Write up for BRBF building*”, Simpson, Gumpertz, & Heger, Inc.: San Francisco, CA.
- Sabelli, R. (2001), “Research on improving the design and analysis of earthquake-resistant steel braced frames”, *The 2000 NEHRP Professional Fellowship Report*, Earthquake Engineering Research Institute, Oakland, CA.
- Saad, G., Najjar S. S. and Saddik, F. (2016), “Seismic performance of reinforced concrete shear wall buildings with underground stories” *Earthquakes and Structures*, 10(4):965–988.
- Sabelli, R., Mahin, S., and Chang, C. (2003), “Seismic demands on steel braced frame buildings with buckling-restrained braces”, *Engineering Structures*, 25, 655–666.
- Tera'n-Gilmore, A. Ruiz-García, J. (2011), “Comparative seismic performance of steel frames retrofitted with buckling-restrained braces through the application of Force-Based and Displacement-Based approaches”, *Soil Dynamics and Earthquake Engineering* 31, 478–490.
- Tsai, K.-C., Hsiao, P.-C., Wang, K.-J., Weng, Y.-T., Lin, M.-L., Lin, K.-C., Chen, C.-H., Lai, J.-W., and Lin, S.-L. (2008), “Pseudo-dynamic tests of a full-scale CFT/BRB frame—Part I: Specimen design, experiment and analysis”, *Earthquake Engineering and Structural Dynamics*, 37, 1081–1098.
- Thomsen, JH, Wallace JW. (2004), “Experimental verification of displacement-based design procedures for slender reinforced concrete structural walls”, *Journal of Structural Engineering*, ASCE 130(4), 618–630.
- Tremblay, R., Degrange G., and Blouin J. (1999), “Seismic rehabilitation of a four-storey building with a stiffened bracing system”, *Proceedings of the 8th Canadian Conference on Earthquake Engineering*, Vancouver, Canada.
- Tremblay, R., Bolduc, P., Neville, R., and DeVall, R. (2006), “Seismic testing and performance of buckling restrained bracing systems”, *Canadian Journal of Civil Engineering*, 33, 183–198.
- Uriz, P., and Mahin, S. A. (2008), “Toward earthquake-resistant design of concentrically braced steel-frame structures”, *PEER 2008/08*, Pacific Earthquake Engineering Research Center, University of California, Berkeley, CA.
- Vafaei, D. and Eskandari, R. (2014), “Seismic response of mega buckling-restrained braces subjected to fling-step and forward-directivity near-fault ground motions”, *The Structural Design of Tall and Special Buildings* 24(9).
- Wu, A.-C., Lin, P.-C., and Tsai, K.-C. (2012), “A type of buckling restrained brace for convenient inspection and replacement”, *Proceedings, 15th World Conference on Earthquake Engineering*, Lisbon.
- Wu, A.-C., Lin, P.-C., and Tsai, K.-C. (2014), “High-mode buckling responses of buckling-restrained brace core plates”, *Earthquake Engineering and Structural Dynamics*, 43, 375–393. Accessed August 2015, <http://onlinelibrary.wiley.com/doi/10.1002/eqe.2349/> abstract, doi: 10.1002/eqe.2349.
- Watanabe, A., Hitomi, Y., Saeki, E., Wada, A., and Fujimoto, M. (1988), “Properties of brace encased in buckling-restraining concrete and steel tube,” *Proceedings of the 9th World Conference on Earthquake Engineering*, Tokyo-Kyoto, Japan.
- Watanabe, A. (1992), “Development of composite brace with a large ductility”, *Proceedings of the U.S.-Japan Workshop on Composite and Hybrid Structures*, Berkeley, CA, September 10–12.